Ann. For. Res. 67(1): 143-154, 2024
https://doi.org/10.15287/afr.2024.3636

ANNALS OF FOREST RESEARCH
www.afrjournal.org

Estimating canopy and stand structure in hybrid poplar plantations from multispectral UAV imagery

Elio Romano[1], Massimo Brambilla[1], Francesco Chianucci[2], Clara Tattoni[3,4], Nicola Puletti[2], Gherardo Chirici[4,5], Davide Travaglini[4,5], Francesca Giannetti[4,5] ✉

Romano E., Brambilla M., Chianucci F., Tattoni C., Puletti N., Chirici G., Travaglini D., Giannetti F., 2024. Estimating canopy and stand structure in hybrid poplar plantations from multispectral UAV imagery. Ann. For. Res. 67(1): 143-154.

Abstract Accurate estimates of canopy structure like canopy cover (CC), Leaf Area Index (LAI), crown volume (Vcr), as well as tree and stand structure like stem volume (V_st) and basal area (G), are considered essential measures to manage poplar plantations effectively as they are correlated with the growth rate and the detection of possible stress. This research exploits the possibility of developing a precision forestry application using an unmanned aerial vehicle (UAV), terrestrial digital camera and traditional field measurements to monitor poplar plantation variables. We set up the procedure using explanatory variables from the Grey Level Co-occurrence Matrix textural metrics (Entropy, Variance, Dissimilarity and Contrast) calculated based on UAV multispectral imagery. Our results show that the GCLM texture derived by multispectral ortomosaic provides adequate explanatory variables to predict poplar plantation characteristics related to plants' canopy and stand structure. The evaluation of the models targeting the different poplar plantation variables (i.e. Vcr, G_ha, Vst_ha, CC and LAI) with the four GLCM explanatory variables (i.e. Entropy, Variance, Dissimilarity and Contrast) consistently higher or equal resulted to $R^2 \geq 0.86$.

Keywords: canopy structure; poplar plantation; texture metrics, GCLM metrics, digital camera, unmanned aerial vehicle, canopy photography.

Addresses: [1]CREA - Council for Agricultural Research and Economics, Research Centre for Engineering and Agro-Food Processing, Treviglio (BG), Italy | [2]CREA - FL, Council for Agricultural Research and Economics, Research Centre for Forestry and Wood, Arezzo, Italy | [3]DiSTA - Dipartimento di Scienze Teoriche ed Applicate, Università degli Studi dell'Insubria, Varese, Italy | [4]Geolab Laboratory of Forest Geomatics, Department of Agriculture Food Environment and Forestry, University of Florence, Florence, Italy | [5]ForTech Laboratorio Congiunto, University of Florence, Florence, Italy.

✉ **Corresponding Author:** Francesca Giannetti (francesca.giannetti@unifi.it).

Manuscript: received April, 10, 2024, revised June 26, 2024; accepted June 27, 2024.

Introduction

In Europe, poplar plantations are strategically important for wood production (FAO 2016) due to poplar plywood's lightweight nature and excellent mechanical properties, which is in high demand across various industries (European Panel Federation 2021). In Europe, wood panel production from poplar plantations is estimated at 627.000 m^3 $year^{-1}$ (European Panel Federation 2021). Furthermore, poplar plantations have been recognized as essential natural-based solutions to mitigate climate change. In fact, poplar trees have a fast-growth rate, enabling them to stock a large amount of CO_2 within a short time (Chen et al. 2019, European Panel Federation 2021, Liu et al. 2022). In addition, poplar plantations are an important asset to conserving and creating ecological networks, which is also pivotal to reducing soil erosions (Zhang et al. 2020, Cantamessa et al. 2022, Vaglio Laurin et al. 2022).

At the European level, Italy has one of the largest areas of produced-oriented poplar plantation, estimated to be 48.639 ha in 2017 and 51.846 ha in 2018 (Zanuttini et al. 2021), with an annual volume of timber given to the supply chain of 2.25 million m^3 whose derived products represent 45% of Italian wood market (D'Amico et al. 2021). Most of the Italian poplar plantations are in the northern part of the Po Valley and are predominantly monospecific. Such plantations have a fast growth rate and a short rotation period of 9-12 years (Zhang et al. 2020, Cantamessa et al. 2022, Vaglio Laurin et al. 2022).

Compared to other EU countries, poplar plantations in Italy are irrigated, as the Italian regulation categorized them as croplands, allowing for pesticides and fertilizers. However, in the last years, due to the increasing drought events in the Po Valley (Baronetti et al. 2022, Romano et al. 2022), and growing concerns about reducing agriculture pollution (Raffaelli et al. 2020) the need to decrease the input for poplar cultivation has emerged. In this context, it has become imperative to develop new easy-to-use continuous monitoring systems that assist poplar owners in detecting the onset of potential plant stress and monitoring the growth rate of the trees and stands.

In today's context, adopting precision forestry tools for managing poplar plantations is highly desirable (Kovacsova & Antalova 2010, Fardusi et al. 2017, Hamrouni et al. 2022). These new instruments offer the potential to update and develop advanced monitoring systems, providing precise estimation of various poplar variables at both stand and tree levels (Dash et al. 2016, Sun et al. 2016, Fardusi et al. 2017, Menéndez-Miguélez et al. 2023). Timely and accurate monitoring of poplar plantations is essential (Meroni et al. 2004, Pu et al. 2021, Cantamessa et al. 2022).

Among the various poplar plantation variables, precise estimates of canopy characteristics such as canopy cover (CC), Leaf Area Index (LAI), Crown Volume (Vcr), as well as tree and stand structure like stem volume (V_st) and basal area (G), are of fundamental importance for effective poplar plantation management. These variables directly impact the growth rate and the occurrence of poplar stress (Gago et al. 2015, Li et al. 2023). Recent studies have highlighted a strong correlation between tree growth and both stem and canopy structures (Wang et al. 2023, Li et al. 2023). For instance, LAI significantly correlates with biomass production, making it a crucial variable for monitoring poplar tree growth under varying water conditions. However, traditional field methods for measuring these variables suffer from limited repeatability due to their cost and time-consuming nature (Peña et al. 2018).

Remote sensing imagery is crucial in scaling up the *in situ* approach. Satellite remote sensing imagery offers the advantage of broader geographical coverage. However, its spatial and temporal resolution is often inadequate for applications focusing on individual tree or stand. In such cases, digital cameras can prove

invaluable in creating innovative monitoring systems. They have the capacity to provide highly detailed information about tree and stand structures, capturing images from the ground (terrestrial photography) and the top canopy using unmanned aerial vehicles (UAVs).

Peña et al. (2018) demonstrated that by using a conventional RGB and a multispectral camera, it was possible to accurately obtain the tree height (RSME=0.21 m) and biomass (RMSE=0.23 kg/m^3). Pu et al. (2021), combining hemispherical photography and UAV-LiDAR data, achieved highly precise results (RMSE=0.053) for canopy closure estimation. Hosingholizade et al. (2023) used slope corrected shadow length and canopy maximum (CM) filtering to determine the heights of pine trees in a forest plantation on RGB UAV imagery and reached solid results, especially with the CM algorithm.

The affordability and ease of managing photogrammetric images with standard software workflows have made consumer-grade RGB and professional multispectral cameras the most commonly used devices among the various payloads that can be installed on UAVs (Ecke et al. 2022, Nex et al. 2022).

Furthermore, photogrammetric data provide the opportunity to extract a large number of explanatory variables from both 3D data (high point clouds metrics and Digital Surface Model (DSM) metrics) and 2D data (including RGB and multispectral orthomosaic values, specific bands values, and vegetation indices, as well as texture features) (Giannetti et al. 2020). Texture features are highly valuable among the numerous explanatory variables derived from photogrammetric data (Nex & Remondino 2014, Bourgoin et al. 2020). Among the multitude of image textures, the Grey Level Co-occurrence Matrix (GLCM) (Dmitriev et al. 2021) is the most used, as it allow the extraction of features that analysed the distribution of grey levels across adjacent pixels, taking into account the spatial position of these pixels within an image or a portion (Humeau-Heurtier 2019). Several studies have demonstrated the utility of GLCM in tasks such as segmenting individual trees (Samal et al. 2006; Bohlin et al. 2012; Onishi and Ise 2021; Khorrami et al. 2022), predicting and estimating forest growing stock volume and structure indices (Bohlin et al. 2012, Giannetti et al. 2020), and identifying leafless poplar plantations (Onishi and Ise 2021).

In this study, we examined the use of multispectral photogrammetric data collected via UAVs to retrieve canopy and stand attributes at plot-level within hybrid poplar plantations. We developed a methodology that integrates field data and terrestrial digital photos to predict variables related to poplar plantations. Instead of relying on 3D photogrammetric data (such as point clouds and Digital Surface Models), our methodology is designed to utilise only multispectral orthomosaics and Grey Level Co-occurrence Matrix (GLCM) features, which are easily manageable by poplar plantation managers. In this approach, in-situ canopy and stand measurements were employed to calibrate the aerial data, making it applicable at broader spatial and temporal scales.

Materials and Methods

Study area

Data were collected in three poplar plantation farms in the Lombardy Region, Northern Italy: Boretto, Torre d'Oglio, and Pomponesco (Figure 1). A total of 51 square plots, 2500 m^2 ha in size each, were selected in hybrid poplar plantations, ranging between 4 to 12 years in age. The tree spacing in the plots varied between 36 m^2 (6x6 m) to 49 m^2 (7x7 m). The location of each plot was georeferenced using a GNSS receiver, and the recorded GNSS data underwent post-processing up to centimetre precision with correction data from a base station. All the data, including forest inventory, terrestrial digital photography and UAV photogrammetric data, were collected simultaneously (i.e. the same day) to prevent potential incongruences.

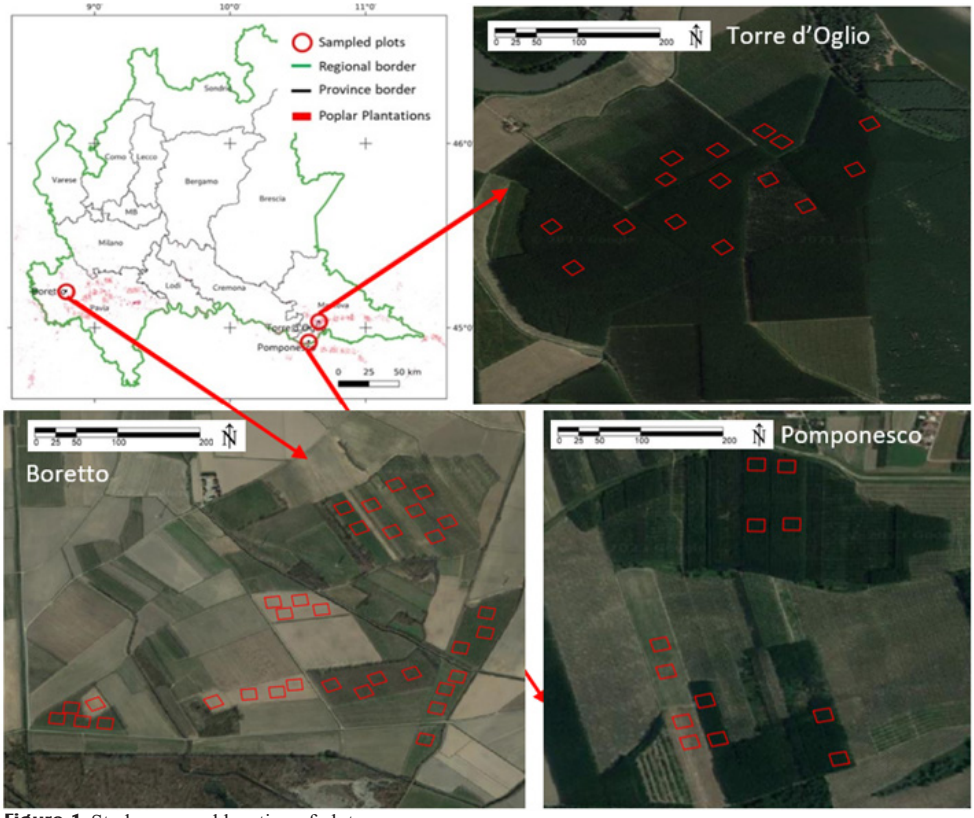

Figure 1 Study area and location of plots.

Forest inventory data

In each plot, the diameter at breast height (D, *m*) of all poplar trees was measured using a calliper, while the tree height (H, *m*) was derived from D using poplar plantation allometric equations derived in an independent study (Chianucci et al. 2020). For each callipered tree, the mentioned allometric models allowed the estimate of the stem volume (Vst, $m^3\ ha^{-1}$), the crown volume (Vcr, m^3) and the calculation of basal area (G, $m^2\ ha^{-1}$).

Terrestrial Digital Cover Photography data

In each plot, 12-20 digital cover photography (DCP) images (Macfarlane et al. 2007) were acquired under overcast sky conditions along a grid of 16 sampling points using a digital single-lens reflex camera (Nikon D90) fitted with an AF Nikkor 50mm 1:1.8 D fixed lens, which yields a field of view of about 30°. The camera was placed at about 1.3 m height and oriented upward. The camera was set in aperture-priority mode, with the aperture set to F8.0; the exposure was set to underexpose the image by one stop (REV -1) to improve the contrast between sky and canopy pixels (Macfarlane et al. 2014).

Images were then analysed using the R package coveR (Chianucci et al. 2022). The blue channel of the image was imported, and a binary classification was performed using Otsu's method (Otsu et al. 1979). Gaps were further classified into large between-crowns gaps, and small within-crown gaps, using a gap size method that identified as "large" those gaps larger than 1.3% image area, as proposed in another study (Pekin & Macfarlane 2009). From the classified total gap fraction (gT; number of pixels classified as sky over the number of total image pixels) and large gap fraction (gL; number of pixels classified as large gaps over the number

of total image pixels), it is possible to estimate canopy cover attributes like foliage cover (FC), which is the complement of gap fraction (GF), and crown cover (CC), which is the fraction of the pixels that complement the between-crowns gaps. Equations 1, 2 and 3 calculated crown porosity (CP) as the fraction of gaps within the crown tree boundaries:

$$FC=1\text{-}gT \quad (1)$$

$$CC=1\text{-}gL \quad (2)$$

$$CP=1\text{-}FC/CC \quad (3)$$

Finally, LAI, defined as half of the total leaf area per horizontal ground area [44], was calculated from a modified Beer-Lamber law:

$$LAI = -CC\,\frac{\ln(CP)}{k} \quad (4)$$

where k is the extinction coefficient, set to 0.85, assuming a planophile distribution of foliage. The canopy attributes calculated for each image were then averaged at the plot level.

UAV acquisition

A Micasense RedEdge multispectral camera sensor (three visible bands (RGB), and two not-visible spectral bands (red-edge and near-infrared (NIR)) was equipped to an octocopter with eight co-axial propellers "STC_X8_U5" UAV: the total payload of the UAV was 4 kg. The study by Chianucci et al. (2021) provides further details regarding the used UAV and the camera.

The acquisition of the images over the 51 poplar plantations took place at noon with a clear sky and calm atmospheric conditions to reduce and minimise the wind and shadow noise effects. The UAV photogrammetric images were collected in the three study sites on the same days of field data and terrestrial digital photography acquisitions to obtain consistent data.

Before the UAV acquisition, in each site, a minimum of 8 ground control points (GCPs) were marked using 50x50 cm targets and measured with a high-performing topographic GNSS receiver. Each GCP lasted for approximately 15 minutes with a 2-s logging rate. The post-processing revealed small deviations in vertical (1.8 cm) and horizontal (0.8 cm) accuracies. The UAV flew at the set altitude of 120 m above ground level, corresponding to a Ground Sampling Distance of 8 cm. The overlap was set to 85% along the tracks and 82% between the tracks: 4 flights covered the whole area. Before each take-off and landing, images of a calibrated reflectance panel were acquired to allow, in the post-processing phase, the conversion of the digital number to reflectance for the abovementioned five bands.

The photogrammetric images acquired with UAV were post-processed using Metashape Agisoft Photoscan. Firstly, the calibration certificate of the reflectance panels was used to convert each band pixel into reflectance for all the images. Then the processing foresaw: (a) image alignment, (b) mesh building, (c) guided marker positioning and optimisation of camera alignment using GCPs (georeferencing of the created scene), (d) dense cloud generation, (e) raster grid DSM generation with a ground resolution of 0.5 m× 0.5 m, and (f) ortomosaic generation at 0.08 m resolution.

Methodology of extraction of explanatory variables from UAV

The high resolution of multispectral ortomosaic acquisitions from UAV imagery data allowed to efficiently perform a Simple Linear Iterative Clustering (SLIC) algorithm for generating superpixels. The SLIC aimed to delineate the individual tree poplar crowns automatically. The use of the SLIC algorithm resulted from its ability to detect poplar plantations accurately (Dmitriev et al. 2021). The SLIC relied on using the Red-Edge multispectral channel since it was the most accurate in defining the tree crowns.

The segmented images were then processed using the Gray-Level Co-occurrence Matrix (GLCM) to calculate four texture metrics (i.e., entropy, variance, dissimilarity, and contrast) for each segmented tree crown using two different image sizes: 80 and 300 MP.

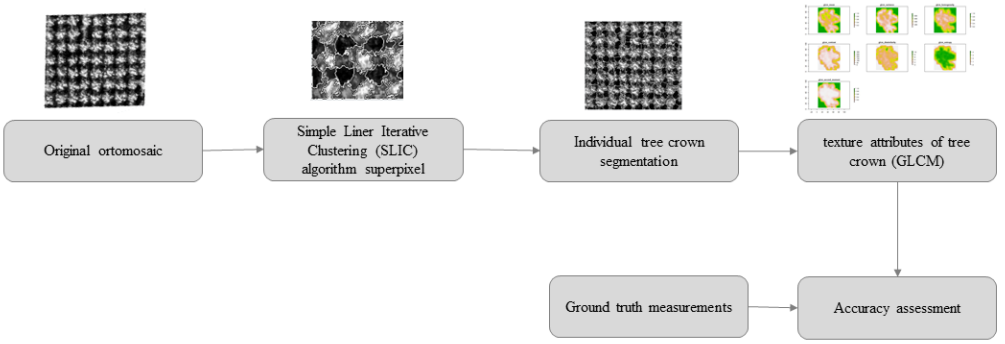

Figure 2 The steps of the used methodology.

The resulting texture metrics derived for each tree were afterwards used as explanatory variables in the model calibration. Figure 2 reports the methodology used with the explained steps. All the methodology was set up using the R software OpenImageR (Mouselimis 2022) package for image management. The superpixels function with the slic method allowed the superpixel preparation; the R glcm package (Haralick et al. 1973, Zvoleff 2020) allowed the research of the statistics using the glcm function.

Liner regression model

A univariate linear regression model was fit between each target poplar plantation variables i.e. forest inventory variables (G_ha, Vcr, Vst_ha) and digital photos variables (CC and LAI) with the GLCM features derived by multispectral UAV ortomosaic. We choose to use linear regression models since they are considered adequate to predict the target poplar plantation variables from UAV photogrammetric data (Brosofske et al. 2014, Puliti et al. 2015, Giannetti et al. 2020) and easier to use than non-parametric methods such as the K-NN and Random Forest.

The 51 square plots measured in the field were randomly divided into calibration and validation datasets (29 for calibration and 22 plots for validation).

In fitting the univariate linear model, the age of the plantation was considered a dummy variable that could assume two values: 1 if the age of the plantations was smaller or equal to 6 years and 0 for plants older than 6 years.

For each of the plot variables using the calibration dataset, we calculate the model according to:

plot variable = $a \cdot (Plant\ age \leq 6) + b\ GLCM\ feature$

where:

- a and b are the model coefficients;
- plant age as a dummy variable;
- GLCM feature (Entropy, Variance, Dissimilarity and Contrast) calculated at 80 and 300 MP.

The model was then applied to the validation dataset (using UAV GCLM metrics calculated on the segmented crown), and the results were compared against the measured variables in the field. The model performance was calculated using different performance indices such as coefficient of determination (R^2), Mean Absolute Error (MAE), root mean square error (RMSE), Nash-Sutcliffe efficiency (NSE), Percent bias (PBIAS), RMSE-observations standard deviation ratio (RMSE-RSR), and Pearson's correlation coefficient (r) (Moriasi et al. 2007).

Results

The results showed a significant correlation between predicted and measured values of the considered poplar plantation variables (i.e. Vcr, G_ha, Vst_ha, CC and LAI) with R^2 consistently higher or equal to 0.86 (R^2 val.) for all the tested models in the validation dataset (Table 1).

The most accurate predictions for LAI and CC were achieved using GLCM variance, while GLCM dissimilarity yielded better results for G_ha and Vst_ha, and GLCM entropy

performed for Vcr (Table 1). Figure 3 reports the scatterplot representing the accuracy of the most accurate models from which it is possible to observe a close alignment between predicted and observed values in the validation dataset. In fact, it can be noted that the slope of the model lines does not differ significantly from the 1.

The MAE and the RMSE are generally consistent with the standard deviations of the observed values for all the variables (Vcr = 131.2; G_ha = 7.62; Vst_ha = 64.3; CC = 0.23; LAI = 0.64). However, it is worth noting that for CC, the 50% value is lower than the standard deviation of the observed values. The NSEs ranging from

Table 1 Summary of the model's validation indexes for all the considered poplar plantation variables and the four GLCM explanatory variables.

GLCM	Tree variables	Model a	Coef. b	R^2 Cal.	R^2 Val.	MAE	RMSE	NSE	PBIAS	RSR-RMSE	*r*
	Vcr	-208.8	3.81	0.92	0.93	71.48	86.96	0.54	11.16	16.44	0.77
	G_ha	-11.3	0.23	0.94	0.92	4.89	5.65	0.42	-13.29	4.44	0.72
Variance	Vst_ha	-95.1	1.92	0.87	0.92	41.29	47.70	0.42	-13.55	12.89	0.72
	CC*	-0.44	0.01	0.96	0.98	0.07	0.10	0.81	0.26	0.45	0.90
	LAI*	-1.03	0.02	0.92	0.93	0.34	0.42	0.87	-0.19	0.89	0.84
	Vcr	-200.4	4.15	0.92	0.92	75.05	91.68	0.49	-11.68	17.34	0.74
	G_ha	-10.8	0.25	0.94	0.91	5.09	5.89	0.37	-13.85	4.62	0.69
Contrast	Vst_ha	-90.93	2.09	0.94	0.91	42.90	49.65	0.37	-14.10	13.41	0.69
	CC	-0.42	0.01	0.96	0.98	0.08	0.11	0.74	-0.59	0.51	0.87
	LAI	-1.00	0.02	0.90	0.91	0.39	0.48	0.84	0.06	1.03	0.80
	Vcr	-179.5	7.30	0.92	0.92	74.52	89.36	0.51	-3.99	16.90	0.73
	G_ha*	-9.59	0.44	0.94	0.92	4.39	5.20	0.51	-6.26	4.08	0.73
Dissimilarity	Vst_ha*	-80.7	3.69	0.94	0.92	37.0	43.84	0.51	-6.50	11.85	0.73
	CC	-0.36	0.02	0.96	0.94	0.13	0.17	0.40	7.36	0.79	0.71
	LAI	-0.86	0.04	0.90	0.86	0.64	0.59	0.69	9.37	1.27	0.60
	Vcr*	-218.8	5.77	0.92	0.94	68.74	84.27	0.57	-13.43	15.94	0.81
	G_ha	-11.7	0.35	0.94	0.93	4.59	5.59	0.44	-15.50	4.39	0.75
Entropy	Vst_ha	-98.0	2.90	0.94	0.92	38.71	47.23	0.43	-15.75	12.76	0.75
	CC	-0.45	0.01	0.96	0.98	0.08	0.11	0.74	-1.39	0.52	0.86
	LAI	-1.05	0.03	0.90	0.91	0.40	0.51	0.79	-3.25	1.08	0.73

Note: * Indicate the most accurate models. Coef: coefficients.

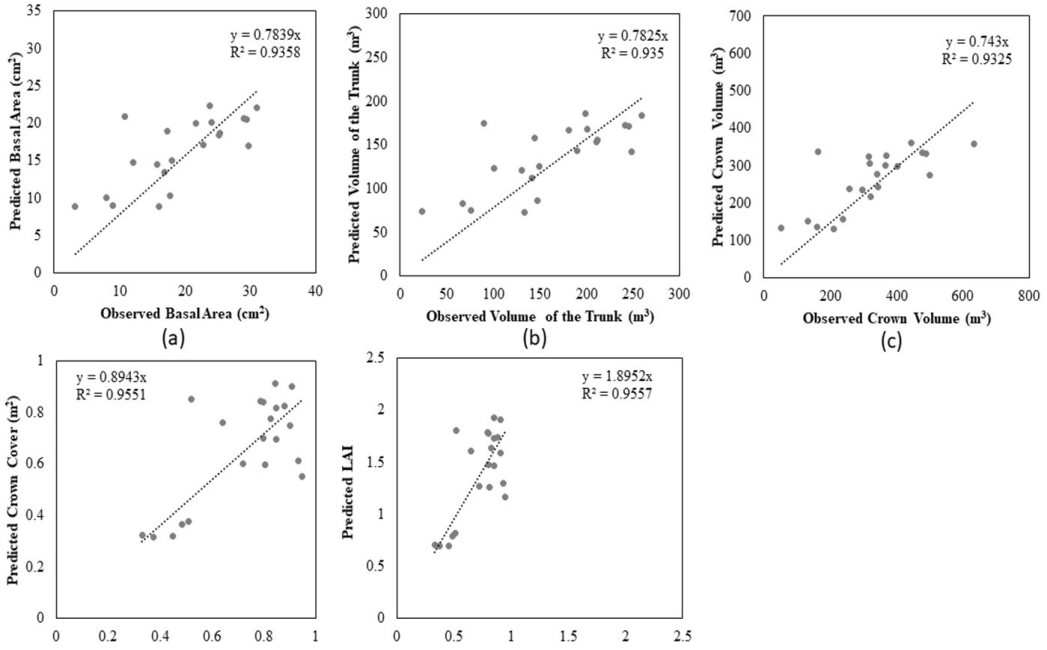

Figure 3 Comparison between predicted and measured variables for the most accurate obtained model for each of the poplar plantation variables considered for the validation dataset.

0.37 to 0.87 across all considered models indicate their adequacy for predictions. In fact, typically, NSE values between 0.0 and 1.0 are considered acceptable levels of performance, while on the contrary, negative indicates unacceptable performance (Nash & Sutcliffe 1970).

The PBIA values consistently align with good performance across all generated models, falling within the acceptable range according to classification standards (±20% as good, <±40% as satisfactory, and >±40% as unsatisfactory) (Ougahi & Mahmood 2022) (Table 1). The Pearson coefficient r ranges from 0.60 to 0.90, indicating a moderate to strong positive correlation between predicted and observed values. CC and LAI are the variables with the highest correlation values, albeit when estimated using contrast and dissimilarity, the relationship weakens. This discrepancy could stem from the mismatch between the GLCM features considered and the plant age groups.

For improved comparability of RMSE values, they were standardized following Loague and Green (Loague & Green 1991) recommendations and evaluated in compliance with the findings of Westermeier and Maidl (Westermeier & Maidl 2019). The standardized RMSE were within the 10-20% for CC, indicating better performance, while for the other variables, the standardized RMSE were always slightly above 30%, indicating less favorable performance.

Discussion

Our results support the idea that GCLM texture features from multispectral ortomosaic are adequate explanatory variables for predicting poplar plantation variables related to crown and stand structure. All the models calibrated with the different target poplar plantation variables (i.e. Vcr, G_ha, Vst_ha, CC, and LAI) and the four GLCM features (i.e. Entropy, Variance, Dissimilarity, and Contrast) calculated based on multispectral UAV ortomosaic resulted in a R^2 val. ≥0.86 (Table 1).

This study confirms that GLCM texture features resulting from high-resolution images are suitable explanatory variables to obtain stem and crown tree variables, confirming the results of other studies (Ozdemir & Karnieli 2011, Ozdemir & Donoghue 2013, Khorrami et al. 2022). In terms of R2, our results were more accurate than those obtained by Ozdemir and Donoghue (2013) in modelling tree diversity index and Giannetti et al. (2020) in modelling forest structure indices. Comparing the results obtained with other Italian studies conducted in forest environments using UAV photogrammetric data, we obtained a RMSE for V_st (RMSE=43.83 m^3/ha), G (RMSE=5.2 m^2/ha) in line with those obtained in Vallombrosa Forest (RMSE Vst = 96.1 m3/ha and G =7.5 m^2/ha) and more accurate results than those obtained in Rincine forest (RMSE Vst = 122.2 m^3/ha and G =12.9 m^2/ha) (Giannetti et al. 2020). These two studies used a larger number of explanatory variables and more complex multivariate linear regression models compared to the one we tested. However, it should be considered that poplar plantations are less complex than the two forests analysed by Giannetti et al. (2020). Comparing our results, with less complex Pinus forest, for crown variables (CC, Vcr, LAI R^2 val ≥ 0.93), we obtained more accurate results in terms of R^2 than those reported by Gülci et al. (2021) in a Turkish Pinus pinea forest (Crown Projection Area R^2=0.89) using 3D RGB photogrammetric UAV, and results in line with those from Lin et al. (2021) achieved in a Chinese Pinus massoniana forests using voxel approach calculated a 3D point cloud derived by oblique photogrammetic UAV flights (LAI, R^2=0.91). Moreover, for G, our results were comparable to those reported for an oil palm plantation using high-resolution FORMOSAT-2 images (G: R^2=0.89) (Migolet and Goïta 2020). In contrast, we obtained more accurate results for Vst compared to the ones reported for the above-ground biomass (R^2=0.68) of a Chinese Pinus elliottii forest resulting from the processing of 3D

photogrammetric UAV data (Song et al. 2022).

Using the Red-Ege band as input, the SLIC method we used to segment the tree crown produced accurate results in detecting the poplar tree crown, even though some of our plots showed considerable under-canopy vegetation (e.g., grass vegetation). It is important to note that under-canopy vegetation may produce noises, affecting the SLIC algorithm and producing less accurate results.

The proposed methodology could be easily applied to obtain wall-to-wall maps of the poplar plantation variables, which can support owners and managers in planning and monitoring the poplar plantations, especially during drought events. Wall-to-wall maps are considered important at the Italian level to develop decisional support systems or early warning systems and are crucial to support the digitalisation of the forest sectors (Fardusi 2017, Giannetti et al. 2020, 2023, Bespalova et al. 2021, Singh et al. 2022). Furthermore, in the case of poplar plantations, these maps can potentially be upgraded with recursive UAV acquisitions, highlighting the importance of future multi-temporal studies.

In the present study, we aimed to develop an accessible methodology using data and models (i.e. ortomosaic and GLCM, univariate linear regression modelling) that poplar plantation owners can easily manage. However, integrating such models with 3D data and non-parametric methods would yield even more accurate results. Additionally, as pointed out by Chianucci et al. (2021) for the canopy variables, the proposed methods can upscale using Sentinel-2 Satellite images since canopy variables are also highly correlated with vegetation indexes calculated at a more coarse scale (i.e. 10 m) compared to UAV data resolution (i.e. 0.08 m). Therefore, canopy photography provides a cost-effective and rapid way to obtain reference canopy variables in situ, which can be used to calibrate metrics from UAV data, where the latter can be used for more routine measurements and monitoring of poplar plantation attributes.

Conclusions

This research highlights the relevance of GLCM textures metrics derived from multispectral UAV ortomosaic as significant explanatory variables for accurately predicting poplar plantation canopy characteristics and stand forest inventory variables using linear regression models. The findings from this study indicate that the proposed approach effectively offers a reliable and efficient alternative to traditional measurement techniques, requiring only a limited number of field plot acquisitions (traditional field and digital photography measures). This method enables comprehensive information gathering across all areas covered by UAV. However, it is important to note that this methodology must be suitable only for application at the farm scale due to the limited operation range of the UAVs. Future research should focus on assessing the accuracy of our methodology using multitemporal UAV acquisitions without the need for field data acquisition.

Author Contributions Conceptualization

FG, FC, ER, and MB; methodology: ER, MB, FG and FC; data acquisition: FG, FC, NP, data curation: FC, CT, NP, FG, ER, MB; formal analysis: ER, MB, FG; writing -original draft preparation: FG, MB, ER, FC; writing -review and editing, NP, CT, GC, DT; supervision: FC, FG; funding acquisition: FC, NP, FG.

Compliance with ethical standards

Conflict of interest

Authors declare there is no conflict of interest.

Funding

The study was funded by the Research Project “Sistema di monitoraggio multiscalare a supporto della pioppicoltura di precisione nella Regione Lombardia” (PRECISIONPOP) funded by the Lombardy region, Italy (grant

number: E86C18002690002). FC was funded by Agritech National Research Center (Piano nazionale di ripresa e resilienza – missione 4 componente 2, CN00000022).

Acknowledgments

We thank the personnel of CREA-Research Centre for Forestry and Wood, for assistance with field data collection.

Data Availability Statement

Data are available on request.

References

Baronetti A., Dubreuil V., Provenzale A., Fratianni S. 2022. Future droughts in northern Italy: high-resolution projections using EURO-CORDEX and MED-CORDEX ensembles. Clim Change 172: 1–22. https://doi.org/10.1007/s10584-022-03370-7

Bespalova V.V., Polyanskaya O.A., Lipinskaya A.A., Gryazkin A.V., & Kazi I.A. 2021. Digital technologies in forestry. In IOP Conference Series: Earth and Environmental Science, 806 (1): 012008. https://doi.org/10.1088/1755-1315/806/1/012008

Bohlin J., Wallerman J., Fransson J.E.S. 2012. Forest variable estimation using photogrammetric matching of digital aerial images in combination with a high-resolution DEM. Scand J For Res 27: 692–699. https://doi.org/10.1080/02827581.2012.686625

Bourgoin C., Betbeder J., Couteron P., et al 2020. UAV-based canopy textures assess changes in forest structure from long-term degradation. Ecol Indic 115: 106386. https://doi.org/10.1016/j.ecolind.2020.106386

Brosofske K.D., Froese R.E., Falkowski M.J., Banskota A. 2014. A review of methods for mapping and prediction of inventory attributes for operational forest management. For Sci 60: 733–756. https://doi.org/10.5849/forsci.12-134

Cantamessa S., Rosso L., Giorcelli A., Chiarabaglio P.M. 2022. Correction: Cantamessa et al. The environmental impact of poplar stand management: a life cycle assessment study of different scenarios. Forests 2022, 13, 464. Forests 13: 1423. https://doi.org/10.3390/f13091423

Chen C., Park T., Wang X., et al. 2019. China and India lead in greening of the world through land-use management. Nat Sustain 2: 122–129. https://doi.org/10.1038/s41893-019-0220-7

Chianucci F., Ferrara C., Puletti N. 2022. coveR: an R package for processing digital cover photography images to retrieve forest canopy attributes. Trees - Struct Funct 36: 1933–1942. https://doi.org/10.1007/s00468-022-02338-5

Chianucci F., Puletti N., Grotti M., et al. 2020. Nondestructive tree stem and crown volume allometry in hybrid poplar plantations derived from terrestrial laser scanning. For Sci 66: 737–746. https://doi.org/10.1093/forsci/fxaa021

Chianucci F., Puletti N., Grotti M., et al. 2021. Influence of image pixel resolution on canopy cover estimation in poplar plantations from field, aerial and satellite optical imagery. Ann Silvic Res 46: 8–13. https://doi.org/10.12899/asr-2074

D'Amico G., Francini S., Giannetti F., et al. 2021. A deep learning approach for automatic mapping of poplar plantations using Sentinel-2 imagery. GIScience Remote Sens 58: 1352–1368. https://doi.org/10.1080/15481603.2021.1988427

Dash J., Pont D., Watt M., et al. 2016. Remote sensing for precision forestry. NZ J For 15–24.

Dmitriev E.V., Kondranin T.V., Melnik P.G., Donskoy S.A. 2021. Statistical texture analysis of forest areas from very high spatial resolution satellite images. CEUR Workshop Proc 3006: 56–66. https://doi.org/10.25743/sdm.2021.64.23.009

Ecke S., Dempewolf J., Frey J., et al. 2022. UAV-Based Forest Health Monitoring: A Systematic Review. Remote Sens 14: 1–45. https://doi.org/10.3390/rs14133205

European Panel Federation, 2021. European poplar and poplar plywood industry: a multi-tool to tackle the climate change and to contribute to the achievement of the objectives of the European Green Deal.

FAO, 2016. Poplars and other fast-growing trees - Renewable resources for future green economies. Synthesis of country progress reports. 25th Session of the International Poplar Commission, Berlin, Federal Republic of Germany, 13-16 September 2016. Working Paper IPC. In: Poplar 25th Session of the International, Commission (eds).

Fardusi M.J., Chianucci F., Barbati A. 2017. Concept to Practices of geospatial information tools to assist forest management and planning under precision forestry framework: a review. 41: 3–14. http://dx.doi.org/10.12899/asr-1354

Gago J., Douthe C., Coopman R.E., et al. 2015. UAVs challenge to assess water stress for sustainable agriculture. Agric Water Manag 153: 9–19. https://doi.org/10.1016/j.agwat.2015.01.020

Giannetti F., Laschi A., Zorzi I., et al. 2023. Forest sharing ® as an innovative facility for sustainable forest management of fragmented forest properties: First results of its implementation. Land 12(3): 521. https://doi.org/10.3390/land12030521

Giannetti F., Puliti S., Puletti N., et al. 2020. Modelling forest structural indices in mixed temperate forests: comparison of UAV photogrammetric DTM-independent variables and ALS variables. Ecol Indic 117: 106513. https://doi.org/10.1016/j.ecolind.2020.106513

Gülci S., Akay A.E., Gülci N., Taş İ. 2021. An assessment of conventional and drone-based measurements for tree attributes in timber volume estimation: A case study on

stone pine plantation. Ecol Inform 63: 101303. https://doi.org/10.1016/j.ecoinf.2021.101303

Haralick R.M., Shanmugam K., Dinstein I. 1973. Textural Features for Image Classification.

Hamrouni Y., Paillassa E., Chéret V., Monteil C., & Sheeren D. 2022. Sentinel-2 poplar index for operational mapping of poplar plantations over large areas. Remote Sensing, 14(16), 3975. https://doi.org/10.3390/rs14163975

Hosingholizade A., Erfanifard Y., Alavipanah S.K., Latifi H., & Jouybari-Moghaddam Y. 2023. Height estimation of pine (*Pinus eldarica*) single trees using slope corrected shadow length on unmanned aerial vehicle (UAV) imagery in a plantation forest. Annals of Forest Research, 66(2): 3-16. https://doi.org/10.15287/afr.2023.3014

Humeau-Heurtier A. 2019. Texture feature extraction methods: A survey. IEEE Access 7: 8975–9000. https://doi.org/10.1109/ACCESS.2018.2890743

Khorrami R.A., Naeimi Z., Wing M., et al. 2022. A new multistep approach to identify leaf-off poplar plantations using airborne imagery. J Geogr Inf Syst 14: 634–651. https://doi.org/10.4236/jgis.2022.146036

Kovacsova P., & Antalova M. 2010. Precision forestry–definition and technologies. Šumarski list, 134(11-12), 603-610.

Li L., Mu X., Jiang H., et al. 2023. Review of ground and aerial methods for vegetation cover fraction (fCover) and related quantities estimation: definitions, advances, challenges, and future perspectives. ISPRS J. Photogramm. Remote Sens. 199: 133–156. https://doi.org/10.1016/j.isprsjprs.2023.03.020

Lin L., Yu K., Yao X., et al. 2021. Uav based estimation of forest leaf area index (Lai) through oblique photogrammetry. Remote Sens 13: 1–17. https://doi.org/10.3390/rs13040803

Liu J., Li D., Fernández J.E., et al. 2022. Variations in water-balance components and carbon stocks in poplar plantations with differing water inputs over a whole rotation: implications for sustainable forest management under climate change. Agric For Meteorol 320: 108958. https://doi.org/10.1016/j.agrformet.2022.108958

Loague K, Green RE (1991) Statistical and graphical methods for evaluating solute transport models: Overview and application. J Contam Hydrol 7: 51–73. https://doi.org/https://doi.org/10.1016/0169-7722(91)90038-3

Macfarlane C, Grigg A, Evangelista C (2007) Estimating forest leaf area using cover and fullframe fisheye photography: Thinking inside the circle. Agric For Meteorol 146: 1–12. https://doi.org/10.1016/j.agrformet.2007.05.001

Macfarlane C, Ryu Y, Ogden GN, Sonnentag O (2014) Digital canopy photography: Exposed and in the raw. Agric For Meteorol 197: 244–253. https://doi.org/10.1016/j.agrformet.2014.05.014

Menéndez-Miguélez M., Madrigal G., Sixto H., Oliveira N. (2023). Calama, R. Terrestrial Laser Scanning for Non-Destructive Estimation of Aboveground Biomass in Short-Rotation Poplar Coppices. Remote Sens. 15: 1942. https://doi.org/10.3390/rs15071942

Meroni M, Colombo R, Panigada C (2004) Inversion of a radiative transfer model with hyperspectral observations for LAI mapping in poplar plantations. Remote Sens Environ 92: 195–206. https://doi.org/10.1016/j.rse.2004.06.005

Migolet P, Goïta K (2020) Evaluation of FORMOSAT-2 and planetscope imagery for aboveground oil palm biomass estimation in a mature plantation in the Congo Basin. Remote Sens 12: 1–24. https://doi.org/10.3390/RS12182926

Moriasi DN, Arnold JG, Liew MW Van, Bingner RL, Harmel RD, Veith TL (2007) Model evaluation guidelines for systematic quantification of accuracy in watershed simulations. Am Soc Agric Biol Eng 50: 885–900. https://doi.org/10.13031/2013.23153

Mouselimis L (2022) OpenImageR: An Image Processing Toolkit.

Nash JE, Sutcliffe J V (1970) River flow forecasting through conceptual models part I — A discussion of principles. J Hydrol 10: 282–290. https://doi.org/https://doi.org/10.1016/0022-1694(70)90255-6

Nex F, Armenakis C, Cramer M, et al (2022) UAV in the advent of the twenties: Where we stand and what is next. ISPRS J Photogramm Remote Sens 184: 215–242. https://doi.org/10.1016/j.isprsjprs.2021.12.006

Nex F, Remondino F (2014) UAV for 3D mapping applications: A review. Appl Geomatics 6: 1–15. https://doi.org/10.1007/s12518-013-0120-x

Onishi M, Ise T (2021) Explainable identification and mapping of trees using UAV RGB image and deep learning. Sci Rep 11: 1–15. https://doi.org/10.1038/s41598-020-79653-9

Otsu N, Smith PL, Reid DB, et al (1979) Otsu_1979_otsu_method. IEEE Trans Syst Man Cybern C: 62–66.

Ougahi JH, Mahmood SA (2022) Evaluation of satellite-based and reanalysis precipitation datasets by hydrologic simulation in the Chenab river basin. J Water Clim Chang 13: 1563–1582. https://doi.org/10.2166/wcc.2022.410

Ozdemir I, Donoghue DNM (2013) Modelling tree size diversity from airborne laser scanning using canopy height models with image texture measures. For Ecol Manage 295: 28–37. https://doi.org/10.1016/j.foreco.2012.12.044

Ozdemir I, Karnieli A (2011) Predicting forest structural parameters using the image texture derived from worldview-2 multispectral imagery in a dryland forest, Israel. Int J Appl Earth Obs Geoinf 13: 701–710. https://doi.org/10.1016/j.jag.2011.05.006

Pekin B., Macfarlane C. 2009. Measurement of crown cover and leaf area index using digital cover photography and its application to remote sensing. Remote Sensing. 1(4): 1298-1320. https://doi.org/10.3390/rs1041298

Peña J.M., de Castro A.I., Torres-Sánchez J., et al. 2018. Estimating tree height and biomass of a poplar

plantation with image-based UAV technology. AIMS Agric Food 3: 313–323. https://doi.org/10.3934/AGRFOOD.2018.3.313

Pu Y., Xu D., Wang H., et al. 2021. Extracting canopy closure by the CHM-based and SHP-based methods with a hemispherical FOV from UAV-LIDAR data in a poplar plantation. Remote Sens 13(19): 3837. https://doi.org/10.3390/rs13193837

Puliti S., Olerka H., Gobakken T., Næsset E. 2015. Inventory of small forest areas using an unmanned aerial system. Remote Sens 7: 9632–9654. https://doi.org/10.3390/rs70809632

Raffaelli K., Deserti M., Stortini M., et al. 2020. Improving air quality in the Po valley, Italy: Some results by the LIFE-IP-PREPAIR project. Atmosphere (Basel) 11 (4): 429. https://doi.org/10.3390/ATMOS11040429

Romano E., Petrangeli A.B., Salerno F., Guyennon N. 2022. Do recent meteorological drought events in central Italy result from long-term trend or increasing variability? Int J Climatol 42: 4111–4128. https://doi.org/10.1002/joc.7487

Samal A., Brandle J.R., Zhang D. 2006. Texture as the basis for individual tree identification. Inf Sci (Ny) 176: 565–576. https://doi.org/10.1016/j.ins.2004.09.017

Singh R., Gehlot A., Akram S.V., Thakur A.K., Buddhi D., & Das P.K. 2022. Forest 4.0: Digitalization of forest using the Internet of Things (IoT). Journal of King Saud University-Computer and Information Sciences, 34(8), 5587-5601. https://doi.org/10.1016/j.jksuci.2021.02.009

Song Z., Tomasetto F., Niu X., et al. 2022. Enabling breeding selection for biomass in slash pine using UAV-based imaging. Plant Phenomics 2022: 9783785. https://doi.org/10.34133/2022/9783785

Sun Y., Liang X., Liang Z., Welham C., Li W. 2016. Deriving merchantable volume in poplar through a localized tapering function from non-destructive terrestrial laser scanning. Forests 7(4): 87. https://doi.org/10.3390/f7040087

Vaglio Laurin G., Mattioli W., Innocenti S., et al. 2022. Potential of ALOS2 polarimetric imagery to support management of poplar plantations in Northern Italy. Remote Sens 14: 1–14. https://doi.org/10.3390/rs14205202

Wang J., Jiang L., Xin S., et al. 2023. Two new methods applied to crown width additive models: a case study for three tree species in Northeastern China. Ann For Sci 80: 11. https://doi.org/10.1186/s13595-022-01165-5

Westermeier M., Maidl F.X. 2019. Comparison of spectral indices to detect nitrogen uptake in winter wheat. J fur Kult 71: 238–248. https://doi.org/10.5073/JfK.2019.08-09.02

Zanuttini R., Negro F., Cremonini C. 2021. Hardness and contact angle of thermo-treated poplar plywood for bio-building. IForest 14: 274–277. https://doi.org/10.3832/ifor3662-014

Zhang Y., Tian Y., Ding S., et al. 2020. Growth, carbon storage, and optimal rotation in poplar plantations: A case study on clone and planting spacing effects. Forests 11: 1–15. https://doi.org/10.3390/F11080842

Zvoleff A. 2020. Package 'glcm'.